PHYSICAL REVIEW B **71**, 041310(R) (2005)

Atomic scale observation of a two-dimensional liquid-solid phase transition on the Si(111)-$\sqrt{3}\times\sqrt{3}$-Ag surface

Canhua Liu,* Shiro Yamazaki, Rei Hobara, Iwao Matsuda, and Shuji Hasegawa
Department of Physics, School of Science, University of Tokyo, 7-3-1 Hongo, Bunkyo-ku, Tokyo 113-0033, Japan
(Received 1 July 2004; revised manuscript received 6 December 2004; published 31 January 2005)

Two-dimensional (2D) liquid-solid phase transition was investigated using a model system of a Cs overlayer adsorbed on a Si(111)-$\sqrt{3}\times\sqrt{3}$-Ag surface by scanning tunneling microscopy (STM). Depending on the Cs coverage, the STM images show the overlayer at a liquid state, a solid state, and a state in-between that is identified to be a two-phase coexisting region. Thus, the 2D freezing transition from liquid to solid is pictured on an atomic scale as a nucleation process. The polygon construction of the two-phase coexisting region reveals clearly that the 2D melting transition from solid to liquid proceeds by the mechanism of geometrical defect condensation.

DOI: 10.1103/PhysRevB.71.041310 PACS number(s): 68.37.Ef, 68.35.Rh, 64.70.Dv, 64.60.Qb

Melting and freezing of matter are among the most common yet fascinating physical phenomena. History of the study stretches back more than 100 years.[1] Because of the topological simplification (fewer neighbors) relative to three dimensions, two-dimensional (2D) systems have provided a fertile medium for studying the phase transitions. Considerable theoretical and computational progresses have led to a number of mechanisms proposed for 2D melting.[2,3] However, no generally accepted understanding has emerged yet. One of the 2D melting mechanisms noticed here is geometrical defect condensation (GDC), which was proposed by Glaser and Clark based on their simulation works.[2,4]

The GDC mechanism offers a developed way, so-called a polygon construction, to depict the structure of a 2D system during melting. The polygon construction is based on the nearest-neighbor bond network (identified with a Voronoi construction[5]), and is formed by removing bonds that are significantly longer than the most probable nearest-neighbor separation. In a 2D solid phase, the polygon construction displays a hexagonal network with atoms residing on the vertices. In a 2D liquid or a two-phase coexisting state, however, the network consists of polygons having three or more sides. The polygons with more than three sides are regarded as geometrical defects, representing localized and easily identified deviations from the hexagonal packing. According to the GDC mechanism, the geometrical defects are particle-like excitations having anisotropic and attractive interactions with each other. Such attractive interactions cause the defects to aggregate into characteristic structures. And, if the interaction is sufficiently strong, it can lead to a first-order condensation transition from a solid phase containing few geometrical defects into a liquid phase containing a high density of the defects. Three-dimensional (3D) melting is also suggested to be similar to the 2D melting scenario the GDC mechanism depicts.[2]

However, the GDC mechanism has not had any supporting experimental evidence yet. One of the reasons is that drawing the polygon construction for a 2D system requires a direct observation of the topography in real space. A large number of experiments on the 2D systems of adsorbed overlayers, such as various gases adsorbed on graphite[6] and metals on metals,[7,8] have been performed in order to probe the nature of the 2D melting transition. But all of such 2D adsorbed overlayers were investigated mainly in reciprocal space by x-ray or electron diffraction, which could not offer a clear and direct view, especially for the inhomogeneous local structures during the melting process.[7,9] The emergence of scanning tunneling microscope (STM) allows us to visualize the arrangement of individual atoms on material surfaces in real space. This makes it possible to observe directly the topography of a 2D system in melting on an atomic scale with STM, so that the polygon construction may be drawn easily.

In this paper we report observations of Cs overlayers adsorbed on a surface of Si(111)-$\sqrt{3}\times\sqrt{3}$-Ag ($\sqrt{3}$-Ag in short hereafter) using STM to study the characteristics of 2D melting in real space and on atomic scale. The substrate of $\sqrt{3}$-Ag surface is induced by one monolayer [(ML), 1 ML equals 7.8×10^{14} cm^{-2}, the density of the most top Si atoms in the ideal Si(111)-1×1 surface] of Ag adsorption on a Si(111) crystal.[10] We have chosen this surface as the substrate mainly because it is atomically smooth without any dangling bonds left, so that the interaction between the substrate and the adatoms on top of it is known to be very weak.[10] The STM images clearly reveal that, by changing the Cs coverage, the overlayer induces a 2D liquid-solid phase transition. By analyzing the distribution of Cs adatoms in the process of melting by the polygon construction, we find that the GDC mechanism is very plausible in explaining the 2D melting transition.

The experiments, including the formation of the Cs overlayers and STM observations, were carried out in an ultrahigh-vacuum chamber with a base pressure of $\sim5\times10^{-11}$ Torr. The details are found elsewhere.[10–12] After depositing various amounts of Cs atoms onto the substrate at room temperature (RT), the sample was cooled to 65 K for STM observations. It is worth mentioning that at RT, we never found such a liquid-solid phase transition. This is because at RT, the Cs adatoms on the surface of $\sqrt{3}$-Ag have so large a mobility that it is impossible to observe it by STM. Changing the Cs coverage here corresponds to changing the 2D pressure.

Figure 1 shows a series of STM images taken for various Cs coverages on the $\sqrt{3}$-Ag surface. Each bright protrusion

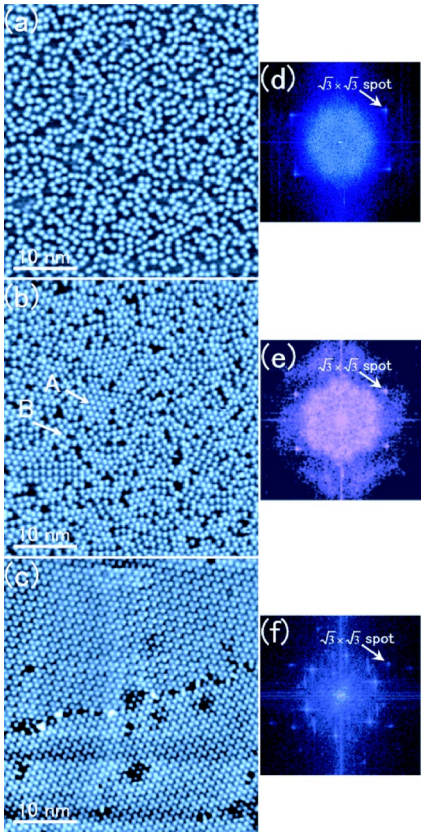

FIG. 1. (Color online) Topographic STM images taken at 65 K for Cs adsorptions on the $\sqrt{3}$-Ag surface with various coverages. $V_{tip}=2.00$ V, $I=0.75$ nA. (a) The liquid phase with Cs coverage of 0.09 ML. (b) The two-phase coexisting region with 0.12 ML. (c) The solid phase with 0.14 ML. (d), (e), and (f) are the Fourier transforms of (a), (b), and (c), respectively.

corresponds to a partially ionized single Cs atom, which has been determined from the size of the protrusion.[12] Alkali metals adsorbed on metal or semiconductor surfaces usually donate electrons to the substrate, causing a characteristic decrease of work function.[13] For our Cs overlayers, similar changes in work function were observed with increasing the Cs coverage. Therefore, the main lateral interaction at small interatomic distances among the Cs atoms may be dipole-dipole type that is repulsive. This is supported by the fact that there are no Cs islands or clusters observed in the STM images. Since, on the other hand, the $\sqrt{3}$-Ag substrate is known to have a metallic surface-state band,[10] an adatom-adatom interaction mediated through the surface-state band may also work at long range.[14,15]

A very small amount of Cs adsorbate (0.01 ML) on the $\sqrt{3}$-Ag surface (not shown here) was found to display no order in atomic arrangement and possess a quite high mobility;[12] every Cs atom moved from frame to frame during STM scanning. This is regarded to be a 2D gas phase. Increasing the coverage up to about 0.09 ML makes the Cs overlayer condense into a 2D liquid phase, whose typical topographic STM image is shown in Fig. 1(a). The Cs atoms in this phase were also movable although the mobility was much lower than in the 2D gas phase;[12] only a few atoms moved from frame to frame. Figure 1(a) displays short-range order in the Cs overlayer, which is more clearly implied by the *halo* pattern in its Fourier transform in Fig. 1(d). Besides the halo, there are six bright spots showing long-range order of $\sqrt{3}\times\sqrt{3}$, which originates from the $\sqrt{3}$-Ag substrate. By comparing the halo pattern with the $\sqrt{3}\times\sqrt{3}$ spots, we calculated the average interatomic distance among the Cs atoms to be 1–1.15 nm.

When the Cs coverage is increased to about 0.12 ML, the STM image in Fig. 1(b) is quite different from Fig. 1(a); there are several discrete regions (indicated by capital *A*) composed of hexagonal lattices, separated by disordered regions (indicated by capital *B*). Its Fourier transform [Fig. 1(e)] also displays a halolike pattern, which, however, is not completely circular in shape, but appears with a hexagon hiding in it. The hiding hexagon comes from an order of $\sqrt{7}\times\sqrt{7}$, which lies in the hexagonal lattice regions with an average interatomic distance of ~1.02 nm, a similar value in the liquid phase [Fig. 1(a)].

Increasing the Cs coverage further up to about 0.14 ML makes the Cs overlayer condense into a pure 2D solid phase that possesses long-range translational order as shown in Fig. 1(c). The Cs adatoms arrange in the hexagonal lattice with order of $\sqrt{7}\times\sqrt{7}$. But, because of the substrate of $\sqrt{3}$-Ag surface, the 2D solid phase has an order of $\sqrt{21}\times\sqrt{21}$ with respect to the Si(111) substrate, named by the Si(111)-$\sqrt{21}\times\sqrt{21}$-(Ag+Cs) surface superstructure. It has double domains rotated by 21.78° to each other. Its long-range translational order is evident with the discrete spots in the Fourier transform [Fig. 1(f)].

More evidence for the assignments we have made of the liquid and solid phases in Figs. 1(a) and 1(c) is derived from an analysis of the bond orientational correlation function:[16] $g_6(r)=\langle\psi_6(\mathbf{r})\psi_6(\mathbf{0})\rangle$ with $\psi_6(\mathbf{r}_l)=(1/n_l)\Sigma_j^{n_l}\exp\{6i\theta_{lj}(\mathbf{r}_l)\}$, where $\theta_{lj}(\mathbf{r}_l)$ is the orientation of the nearest-neighbor bond between atom l and its jth neighbor relative to an arbitrary direction. n_l is the number of the nearest neighbors of atom l located at $\mathbf{r}_l$. The calculation results for the STM images in Fig. 1 are displayed in Fig. 2, from which we see that $g_6(r)$ in the liquid phase [Fig. 2(a)] decays exponentially with increasing atomic separation r (nm) as $\sim\exp(-r/0.65)$, while in the solid phase [Fig. 2(c)] it does not decay in a single domain.

Next we characterized the state between the liquid and solid phases, shown in Fig. 1(b). We calculated its $g_6(r)$, and again found it to decay exponentially as $\sim\exp(-r/1.70)$ as shown in Fig. 2(b).[17] Such a decaying is a typical behavior of the bond orientational correlation function in a liquid state. However, we do not think of it as a pure liquid phase since its $g_6(r)$ decays much more slowly than that in a pure liquid phase in Fig. 2(a). In addition, it appears inhomogeneous as discovered in the STM image in Fig. 1(b). This idea was proved by a further analysis of the angular susceptibility χ_6, which is defined by $\chi_6=\langle|(1/N)\Sigma_l\psi_6(\mathbf{r}_l)|^2\rangle$, where N is the total number of atoms.

We follow Strandburg *et al.*[9] to use this quantity to examine the system on different length scales by dividing the image of Fig. 1(b) into subsystems of smaller squares with areas of $1/(4\times4)$, $1/(16\times16)$, and $1/(32\times32)$ of the whole STM image. For a pure liquid phase, χ_6 should be small for

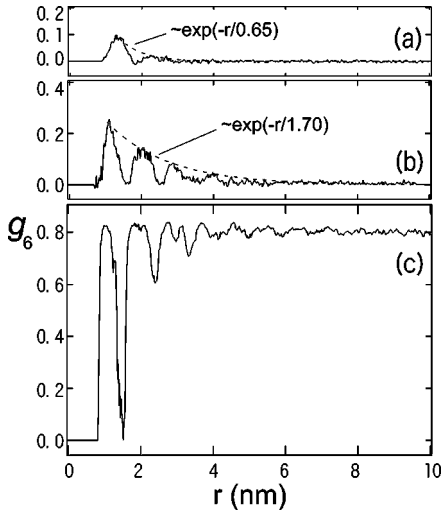

FIG. 2. Bond orientational correlation functions for (a) the liquid phase, (b) the two-phase coexisting state, and (c) the solid phase, each of which is calculated from three STM images similar to those shown in Figs. 1(a)–1(c), respectively.

lack of translational order for all length scales, while it should be large in a solid phase for all sizes of subsystems. We see from Fig. 3, however, that with decreasing the size of subsystem, the probability to find subsystems having large χ_6 values becomes larger. This means that there are local areas having a translational order, while such an order does not grow to large domains. The distribution of χ_6 thus can be modeled by a combination of solid and liquid distributions. Hence we conclude that the phase in Fig. 1(b) exhibits an inhomogeneous two-phase coexisting state. The areas having a hexagonal-lattice order locally are in a solid phase, while the disordered areas in-between are in a liquid phase.

With this conclusion we can expect that increasing the Cs density from the liquid phase makes the areas of hexagonally ordered domains grow gradually, which is the process of nucleation and growth in 2D freezing transitions. Conversely, decreasing the Cs density from the solid phase makes the disordered areas grow, which is the 2D melting transition.

Here we follow Glaser and Clark[2,4] to draw the polygon construction from our STM images to depict such a two-

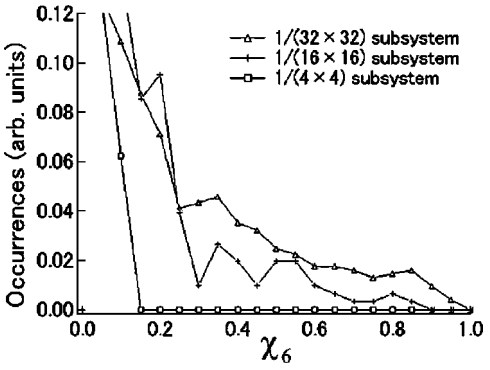

FIG. 3. Angular susceptibility calculated for the STM image of Fig. 1(b).

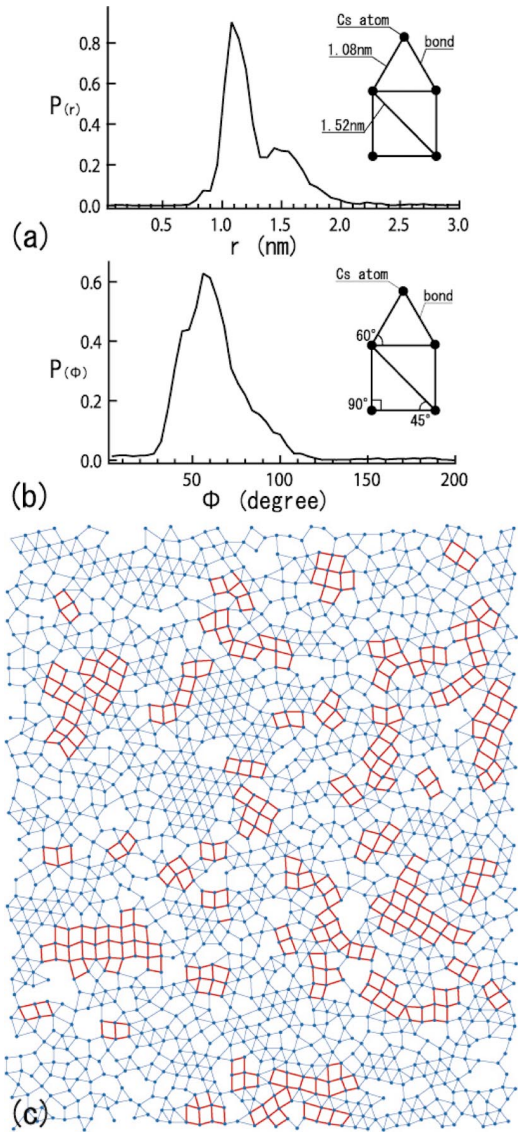

FIG. 4. (Color) Analysis on the two-phase coexisting state of the STM image in Fig. 1(b). (a) Probability distribution of the nearest-neighbor bond lengths r. (b) Probability distribution of the angles between the nearest-neighbor bonds Φ. (c) Polygon construction.

phase coexisting region. Figure 4(a) displays the distribution $P(r)$ of the nearest-neighbor bond lengths $r \equiv r_{lj}$, and Fig. 4(b) shows the distribution $P(\Phi)$ of angles $\Phi \equiv \Phi_{lj} = \theta_{l,j+1} - \theta_{l,j}$ between adjacent nearest-neighbor bonds, calculated from Fig. 1(b). In Fig. 4(a) the spectrum has two peaks at $r = 1.08$ and 1.52 nm. It is noticed that $1.52/1.08 = 1.407 \sim \sqrt{2}$, which is the length of the diagonal line of a unit square. The spectrum in Fig. 4(b) appear to have three peaks at $\Phi = 45°$, 58° and 90°, and their origins are shown in the inset. Thus, these two spectra strongly indicate the existence of "square" lattices besides the hexagonal lattices.

By removing the nearest-neighbor bonds longer than 1.35 nm, which corresponds to a valley in the spectrum in Fig. 4(a), we draw the polygon construction in Fig. 4(c). It is easy to identify local square lattices, which are defined with other polygons as geometrical defects. The interesting thing is that the square geometrical defects aggregate into ladder-

like clusters, which are distinguished by red, thick-line bonds in Fig. 4(c). As a distinctive characteristic, these ladderlike clusters of "square" lattices also exist in Glaser and Clark's simulation results. The real-space observations here thus agree well with the GDC mechanism. Therefore, it is reasonable to believe that the 2D melting occurs through the proliferation of geometrical defects (local "square" particle arrangement), which aggregate into characteristic local structures (ladderlike clusters) during the process of 2D melting.

Although the results of the STM observations agree well with the simulation result of GDC mechanism, it must be noted that the substrate on which the 2D melting occurs in the experiment is not so smooth as that used in the simulation, since all Cs adatoms sit on well-defined adsorption sites in the $\sqrt{3}$-Ag unit cell.[12] But this difference should not make any essential change in the conclusion because the characteristics of 2D melting transition displayed by STM observations is due to the interaction within the Cs overlayer, not due to the lattice of the substrate. The substrate may induce discrete values of the nearest-neighbor distances and bond angles given by the substrate lattice vectors, but may not induce the ladderlike clusters of "square" lattices as expected by the GDC mechanism because of the threefold symmetry of the substrate lattice. If the substrate lattice of $\sqrt{3}$-Ag surface has a dominant effect on the phase transition of Cs overlayer, it should allow the smallest interatomic distance among Cs atoms to be 0.665 nm, which is the length of the $\sqrt{3}$-Ag surface unit cell. However, it is obvious from Fig. 4 that this distance is forbidden. Another fact indicating that the substrate lattice has little effect on the 2D melting transition is that the Cs adatoms on the substrate can move (or say, hop) nearly freely in the gas phase even at 65 K, which indicates that the migration potential corrugation on the substrate should be roughly less than 8.4 meV, the kinetic energy of a free Cs atom with three degrees of freedom at 65 K. This is much smaller than the dipole-dipole interaction among the Cs adatoms (several tens meV at least with a Cs separation of 1 nm). Therefore we can say that the observed phase transition is governed dominantly by the adatom-adatom interaction, not by the adatom-substrate interaction.

When discussing the 2D melting mechanism, it is worth mentioning another mechanism called the Kosterlitz-Thouless-Halperin-Nelson-Young (KTHNY) theory,[18–20] because it has attracted and stirred a lot of interest by studying the 2D melting transition during the past 30 years. The KTHNY theory predicts that the 2D solid undergoes a continuous melting transition via the unbinding of dislocations into a hexatic phase, which then undergoes the second transition to the equilibrium liquid via the unbinding of disclinations. In our experiment, however, no such hexatic phase between the solid and liquid states in melting was observed. But it is still difficult to deny it since Nelson and Halperin[20] demonstrated that the KTHNY scenario occurs only for 2D systems on smooth substrates without periodic potential corrugations. In our 2D system of Cs overlayers on the $\sqrt{3}$-Ag surface, the effect of the periodic potential from the substrate could not be ignored although it is not a dominant factor. In addition, another fact preventing us from discussing the experimental results with the KTHNY theory is that what we changed during the phase transition was the Cs coverage, which is a density variable, so it is inevitable that there is a coexistence region associated with a first-order transition.

In summary, we have succeeded in making an atomic-scale observation of the 2D liquid-solid phase transition in real space. By drawing the polygon construction for the two-phase coexisting region, we provided strong evidence for the GDC mechanism in explaining the 2D melting transition in this particular system.

This work has been supported by a Grants-In-Aid from the Japanese Society for the Promotion of Science.

*Electronic address: liu@surface.phys.s.u-tokyo.ac.jp

[1] J. G. Dash, Rev. Mod. Phys. **71**, 1737 (1999).
[2] M. A. Glaser and N. A. Clark, Adv. Chem. Phys. **83**, 543 (1993).
[3] K. J. Strandburg, Rev. Mod. Phys. **60**, 161 (1988).
[4] M. A. Glaser and N. A. Clark, Phys. Rev. A **41**, 4585 (1990).
[5] G. F. Voronoi, J. Reine Angew. Math. **134**, 198 (1908).
[6] J. P. McTague, J. Als-Nielsen, J. Bohr, and M. Nielsen, Phys. Rev. B **25**, 7765 (1982).
[7] R. D. Diehl and R. McGrath, Surf. Sci. Rep. **23**, 49 (1996).
[8] W. C. Fan and A. Ignatiev, Phys. Rev. B **37**, 5274 (1988).
[9] K. J. Strandburg, J. A. Zollweg, and G. V. Chester, Phys. Rev. B **30**, 2755 (1984).
[10] S. Hasegawa *et al.*, Prog. Surf. Sci. **60**, 89 (1999).
[11] C. Liu *et al.*, Jpn. J. Appl. Phys., Part 1 **42**, 4659 (2003).
[12] C. Liu, I. Matsuda, and S. Hasegawa, Surf. Interface Anal. (to be published).
[13] H. Ishida, Phys. Rev. B **38**, 8006 (1988).
[14] P. Hyldgaard and T. L. Einstein, Surf. Sci. **532–535**, 600 (2003), and references therein.
[15] N. Knorr, H. Brune, M. Epple, A. Hirstein, M. A. Schneider, and K. Kern, Phys. Rev. B **65**, 115420 (2002), and references therein.
[16] K. Chen, T. Kaplan, and M. Mostoller, Phys. Rev. Lett. **74**, 4019 (1995).
[17] Three STM images almost identical to that in Fig. 1(b) were used for the analysis in order to diminish noise induced by STM resolution. The decay range of ~4 nm in Fig. 2(b) is not surprising when noticing that the particle (adatom) size is only about 0.6 nm. Actually the ratio between the decay range and the particle size here is ~7, which is similar to those displayed in a 2D colloid system in melting transition such as in A. H. Marcus and S. A. Rice, Phys. Rev. Lett. **77**, 2577 (1996); and in C. A. Murray and D. H. van Winkle, *ibid.* **58**, 1200 (1987). In the former reference the ratio is ~5 and in the latter ~10. Therefore, the influence of finite-size scaling may be small here even the scanning scale of the STM images is only about 40 nm.
[18] J. M. Kosterlitz and D. J. Thouless, J. Phys. C **6**, 1181 (1973).
[19] A. P. Young, Phys. Rev. B **19**, 1855 (1979).
[20] D. R. Nelson and B. I. Halperin, Phys. Rev. B **19**, 2457 (1979).